ELSEVIER

Journal of Power Sources 107 (2002) 34–41

JOURNAL OF POWER SOURCES

www.elsevier.com/locate/jpowsour

Structural aspects on the charged positive Ni electrode

Lars Eriksson[a,*], Ulrik Palmqvist[b], Håkan Rundlöf[c], Urban Thuresson[b], Rune Sjövall[b]

[a]*Arrhenius Laboratory, Division of Structural Chemistry, Stockholm University, SE-106 91 Stockholm, Sweden*
[b]*Arrhenius Laboratory, Division of Inorganic Chemistry, Stockholm University, SE-106 91 Stockholm, Sweden*
[c]*Studsvik Neutron Research Laboratory, Uppsala University, SE-611 82 Nyköping, Sweden*

Received 9 July 2001; accepted 15 October 2001

Abstract

X-ray powder diffraction (XPD) and neutron powder diffraction (NPD) measurements in combination with theoretical calculations were performed on discharged and charged positive material of the Ni hydroxide electrode.

The $Ni(OH)_2$ in the battery material is disordered to a large extent and show large contributions of amorphous phases. The results of this investigation indicate similar local structures for the discharged and the charged phases. During charging, the *c*-direction remains essentially unaffected, whereas the *ab*-plane shows a high degree of disorder resulting in the disappearance of the [1 0 0] peak. A NPD pattern was used for indexing and refining of unit cell parameters. A revised conventional unit cell for the charged β-structure is proposed; hexagonal crystal system with $a = 2.98(1)$ and $c = 4.69(7)$ Å. We propose a structural model of the charged phase as consisting of disordered separate domains in the *ab*-plane.

The conventional γ-phase is proposed to constitute of a modification of the β-NiOOH structure and is usually supposed to contain vacancies/defects in the *c*-direction. We show in this paper that the γ-phase may also be interpreted as consisting of partial systematic defects in the *ab*-plane. This phase can be indexed with an orthorhombic cell: $a = 7.50(2)$, $b = 4.83(2)$ and $c = 3.97(1)$ Å, respectively.

Keywords: β-NiOOH; β-$Ni(OH)_2$; γ-Phase; XPD; NPD; RDF; Indexing

1. Introduction

The Ni electrode has been widely investigated over the years since it has been used as the positive electrode in many battery systems. Despite this, there still seems to be more to investigate concerning the charge/discharge mechanism and phase transformations involved. The predominant description of these phases is that of Bode et al. [1]. In Bode's description the discharged phase, β-$Ni(OH)_2$, has the Brucite structure with NiO_2 layers having the ABAB stacking sequence. The hydrogen atoms are bonded to the oxygen atoms and located in between the NiO_2 layers. β-$Ni(OH)_2$ has a hexagonal unit cell: $a = 3.126$ and $c = 4.605$ Å. During charging of β-$Ni(OH)_2$ it transforms to β-NiOOH with preserved ABAB sequence but with slightly changed cell dimensions: $a = 2.81$ and $c = 4.84$ Å. The loss of every second hydrogen results in a contraction of the *ab*-plane due to shorter Ni–O distances, and elongation in the *c*-direction due to increased NiO_2 layer repulsion. Further charging of β-NiOOH gives a new phase, γ-NiOOH, in which both water molecules and alkali metals intercalate between the NiO_2 layers. The unit cell dimensions are claimed to be: $a = 2.82$ and $c \approx 7$ Å. The formula γ-NiOOH is normally used for a number of different compositions of this overcharged phase. A more appropriate formula is $Ni_{1-x}K_xOOH \cdot wH_2O$. On a subsequent discharge the β-$Ni(OH)_2$ phase is regained via an intermediate turbostratic α-$Ni(OH)_2$ phase, which is not stable in concentrated electrolyte.

From structural point of view it is not easy to determine neither the unit cell nor the atom positions in β-$Ni(OH)_2$/β-NiOOH used as battery electrodes due to the low degree of crystallinity of the material and consequently lack of well defined Bragg reflections. A low crystallinity (amorphous) material is, however, desirable in the battery since it means lower impedance during charging/discharging. In order to bring some further light on the crystallography of the Ni electrode, an X-ray powder diffraction (XPD) and neutron powder diffraction (NPD) study in combination with theoretical calculations and radial distribution functions (RDF) has been undertaken on discharged and charged battery materials. Finally, a comparison with synthetically oxidised material was made.

* Corresponding author. Tel.: +46-8-16-2394; fax: +46-8-16-3118.
E-mail address: lerik@struc.su.se (L. Eriksson).

0378-7753/02/$ – see front matter
PII: S0378-7753(01)00984-3

2. Experimental

2.1. Electrical testing

The composition of the Ni hydroxide electrode studied was 80 wt.% β-$Ni(OH)_2$/β-NiOOH and 20 wt.% graphite. The rated capacity was 5 Ah/unit.

The fresh Ni plates were initially subjected to two electrical formation cycles in order to activate the mass. The subsequent discharging and charging cycles were performed at a charge/discharge rate of 0.2 C_5 A and was sampled by a computer controlled system. The capacity of the electrodes were measured at the end voltage of 1.5 V versus a Zn/ZnO reference electrode ($E = -1.3$ V versus SHE).

As counter electrode a thin Ni sheet was used and the electrolyte consisted either of 5.6 M NaOH or by 6.3 M NaOD solution. NaOD was prepared from D_2O (Aldrich, 99.9% D) and Na_2O_2(s) (Merck, p.a.). Na_2O_2 disproportionates according to:

$$O_2^{2-}(aq) \leftrightarrow \tfrac{1}{2}O_2(g) + O^{2-}(aq) \quad (1)$$

The cell container, made of Plexiglas®, was sealed towards the surrounding atmosphere when the NaOD heavy water solution was used as electrolyte.

2.2. Cell dismantling

The cells were dismantled and the electrode material was investigated by XPD and NPD after finished electrical testing. The investigated mass was thereafter washed several times with deionised water and dried at 105 °C. The graphite content was separated after dissolution of the β-$Ni(OH)_2$/β-$Ni(OD)_2$ compounds in 4 M HCl. The fraction of graphite was constant between different samples (21 ± 1 wt.%).

2.3. XPD measurements

The electrode masses were examined by XPD using either a STOE STADI powder diffractometer or a Guinier-Hägg focusing XPD camera (Huber G670a), both using a standard copper sealed tube source and equipped with a Ge monochromator set to diffract Cu $K\alpha_1$($\lambda \approx 1.5405981$ Å).

The measurements using the diffractometer were made at 0.04° intervals in transmission mode over the range 0–134.96° in 2θ using a linear PSD detector covering approximately 6° in 2θ and yielding a total count time of 3400 s per step.

The X-ray diffraction analyses performed on the HUBER G670a image plate Guinier-Hägg camera was made in the 2θ range 4–100° with a step of 0.005°.

2.4. NPD measurements

The NPD measurements ($\lambda \approx 1.47$ Å) were made at 0.08° intervals in transmission mode using a cumulated count time of 100 s for each step over the range 4–140° in 2θ. The measurements were done with the NPD powder diffractometer at NFL, Studsvik, Sweden. The neutron beam was monochromatised with a double crystal Cu(220) monochromator. The multidetector was made of 35 individual detectors (each detector separated 4° in 2θ), giving a total coverage of 140° in 2θ [2].

2.5. Synthesis of β-$Ni(OH)_2$/β-$Ni(OD)_2$ and NiOOH

2.5.1. Synthesis of β-$Ni(OH)_2$/β-$Ni(OD)_2$

An excess of NaOH(aq)/NaOD(aq) was added to a solution of $NiSO_4 \cdot 6H_2O$(aq) (Merck, p.a.) forming β-$Ni(OH)_2$/β-$Ni(OD)_2$. The slurry was washed and centrifuged several times in H_2O/D_2O in order to remove impurities and then dried at ambient temperature.

2.5.2. Synthesis of NiOOH

An excess of NaOCl(s) was added to β-$Ni(OH)_2$ with evolution of gas bubbles that could be interpreted as chlorine gas according to Eq. (2):

$$OCl^-(aq) + Ni(OH)_2(s) \leftrightarrow \tfrac{1}{2}Cl_2(g) + NiOOH(s) + OH^-(aq) \quad (2)$$

Another possible source of the gas evolution is the oxidation of H_2O(l) to O_2(g). The slurry was washed and centrifuged several times in deionised water to remove impurities.

2.5.3. Determination of the degree of oxidation

The total concentration of Ni(III) in the synthesised slurry above was determined, after dissolution in HCl(aq) and addition of an excess of KI(s) (Merck, p.a.), by titration with 0.10 M $S_2O_3^{2-}$(aq) using thiodene as an indicator. An excess of 0.100 M EDTA solution (Merck, p.a.), a NH_4Cl/NH_3 buffer solution and a few drops of the indicator Eriochrome Black T was added to the titrated solution. The solution was back titrated with 0.10 M Zn^{2+}(aq) and the total concentration of Ni in the starting solution was calculated [3]. The ratio between the total concentration of Ni(III) and the total concentration of Ni (the sum of Ni(II) and Ni(III)) was then yielding the degree of oxidation in the starting material.

3. Results and discussion

3.1. XPD measurements

3.1.1. Battery active material

XPD patterns from a discharged and charged positive nickel electrode, which have been charged/discharged 10 times in heavy water alkali solution are shown in Fig. 1. The contributions from graphite, air and tape are subtracted from the diffraction patterns. The high degree of amorphicity in the charged state is clearly shown in the figure displaying smaller peak intensities and increased width of the peaks.

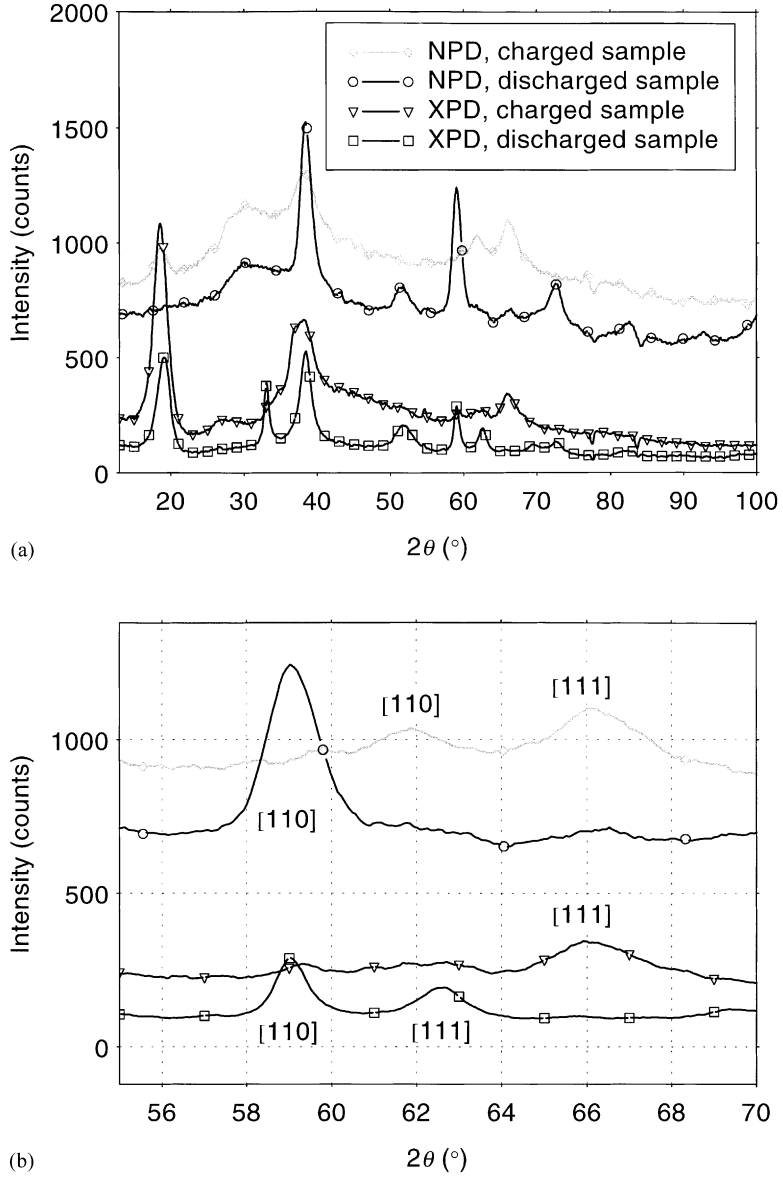

Fig. 1. (a) XPD and NPD patterns from discharged and charged active material (β-Ni(OD)$_2$ and β-NiOOD). The active mass was electrically charged/discharged 10 times in heavy water alkali solution before analysis. The neutron powder patterns were scaled to the same 2θ-scale as the X-ray diffraction patterns. (b) Enlargement of (a) showing the region $2\theta = 55-70°$ with both XPD below and both NPD in above. Indices for discharged patterns are written below and indices for charged pattern above actual pattern.

Salient features of the XPD pattern are that the [1 0 0] peak disappears and the [0 0 1] peak is relatively unaffected by oxidation (charging).

The state of charge of the mass was determined from the discharge capacity measurements and indicated full charge of the electrode material. Neither could any contribution of remaining uncharged material be observed in the diffraction pattern of the charged material.

The main difference between the crystallographic structures of discharged (β-Ni(OH)$_2$) and charged (β-NiOOH) seems to be a dramatic increase of disorder within the *ab*-plane during charging. These results are in accordance with interpretation of EXAFS data [4].

The cell parameters of the discharged phase of the battery material was refined through least-squares calculations [5] from 12 manually estimated peak positions (cf. Table 1) to: $a \approx 3.125(1)$ and $c \approx 4.654(7)$ Å. The elongated c-axis compared to the JCPDS-values (ICDD: 14–0117), $a = 3.126$ and $c = 4.605$ Å can be explained due to the large occurrence of defects in β-Ni(OH)$_2$ [6–8].

The indexing of the charged pattern using only three easily detectable peaks can be performed in several ways with slightly different results. Using the parameters: $a = 2.81$ and $c = 4.84$ Å (ICDD: 6–0141) one can index and refine (with our peak positions) the cell parameters to: $a = 2.826$ and $c = 4.756(3)$ Å. The absence of standard

Table 1
Diffraction data for battery material β-Ni(OH)$_2$ with 12 observed and 12 calculated lines[a]

N	H	K	L	$2\theta_{obs}$	$2\theta_{calc}$	$\Delta 2\theta$
1	0	0	1	19.0653	19.0557	0.0096
2	1	0	0	33.0537	33.0783	−0.0246
3	1	0	1	38.4338	38.4522	−0.0184
4	1	0	2	51.7560	51.7764	−0.0204
5	1	1	0	59.0622	59.0843	−0.0221
6	1	1	1	62.6768	62.6788	−0.0020
7	2	0	0	69.3676	69.4085	−0.0409
8	2	0	1	72.5977	72.7283	−0.1306
9	2	0	2	82.4000	82.3854	0.0146
10	2	1	0	97.8520	97.7309	0.1211
11	2	1	1	100.8514	100.9131	−0.0617
12	2	1	2	110.7723	110.7147	0.0577

[a] Unit cell used to derive the calculated line positions: hexagonal crystal system, $a = 3.125(1)$ and $c = 4.654(7)$ Å. $M(12) = 27.9$, $F(12) = 7.9$ (0.044, 35), $\Delta 2\theta = 2\theta_{obs} - 2\theta_{calc}$.

Table 2
Diffraction data for synthetic β-Ni(OH)$_2$ with14 observed and 19 calculated lines[a]

N	H	K	L	$2\theta_{obs}$	$2\theta_{calc}$	$\Delta 2\theta$
1	0	0	1	18.9402	18.9783	−0.0381
2	1	0	0	33.1454	33.0893	0.0561
3	1	0	1	38.4375	38.4212	0.0163
4	0	0	2		38.5037	−0.0662
5	1	0	2	51.6678	51.6554	0.0124
6	1	1	0	59.0489	59.1052	−0.0563
7	1	1	1	62.5306	62.6706	−0.1400
8	2	0	0		69.4341	0.1991
9	1	0	3	69.6332	69.5983	0.0349
10	2	0	1	72.6970	72.7269	−0.0299
11	1	1	2		72.7806	−0.0836
12	0	0	4	82.5905	82.5146	0.0759
13	2	1	0	97.7721	97.7732	−0.0011
14	2	0	3		97.9285	−0.1564
15	2	1	1	100.9755	100.9301	0.0454
16	1	1	4		110.8709	0.1328
17	0	0	5	111.0037	111.0356	−0.0319
18	3	0	0	117.4106	117.3620	0.0486
19	2	0	4	121.1712	121.2278	−0.0566

[a] Double indexed lines shown with the observed 2θ at the closest calculated position. Unit cell used to derive the calculated line positions: hexagonal crystal system, $a = 3.124(1)$ and $c = 4.672(2)$ Å. $M(14) = 21.8$, $F(14) = 5.8$ (0.059, 41), $\Delta 2\theta = 2\theta_{obs} - 2\theta_{calc}$.

deviation of the a-parameter is due to the fact that it is determined only from one line, indexed as [1 1 0] with this cell. However, we will propose that this line should be indexed as [1 1 1], in the neutron diffraction section (Section 3.2) that give cell parameters more close to the parameters for the discharged phase. The cell parameters extracted from the X-ray diffraction data are: $a = 2.96$ and $c = 4.76$ Å. It is important to realise that these results originate from three broad peaks, which is of course not entirely satisfactory.

3.1.2. Synthesised β-Ni(OH)$_2$ and NiOOH

The appearance of the XPD patterns of synthesised β-Ni(OH)$_2$ and NiOOH is similar to those of the battery materials. All XPD studies were performed on wet samples. A comparison between wet and dried synthesised β-Ni(OH)$_2$ showed, however, identical results.

The cell parameters determined by manually estimated peak positions from synthesised β-Ni(OH)$_2$ are: $a = 3.124(1)$ and $c = 4.672(2)$ Å using 14 peaks (cf. Table 2).

By using the three broad peaks at about 18, 37 and 66° in 2θ of the charged pattern shown in Fig. 2, assuming at this stage that the peaks at about 10 and 25° belongs to the so called γ-NiOOH (ICDD: 6–0075) [9], it is possible to obtain at least two slightly different unit cells, depending on the assignment of indices, with dimensions close to that of the β-phase of the battery material.

3.1.3. The conventional γ-phase

The conventional γ-NiOOH is claimed to exhibit an elongated [0 0 1] direction due to rearrangements, stacking faults and intercalation reactions [7,9–11], giving a c-axis of about 7–8 Å.

The XPD patterns shown in Fig. 2 at time equals 0 after addition of OCl^-(aq) shows a discharged phase. The titration procedure indicated about 5% Ni(III). After 10 min oxidation the XPD pattern indicates that the sample has been transformed to a charged phase. The peaks from the discharged phase disappeared and the conventional γ-peak at about 10° in 2θ has started to show intensity at the same time as the [1 0 0] and [1 1 0] peaks from the β-phase at $2\theta \approx 33$ and 59°, disappears. The β-Ni(OH)$_2$ [0 0 1] peak is essentially unaffected and show a minor shift. The titration experiments indicated about 70% Ni(III) at time equals 1 h. After 6 and 26 h the titration indicated ≥100% Ni(III). Between 1 and 26 h of oxidation the diffraction patterns

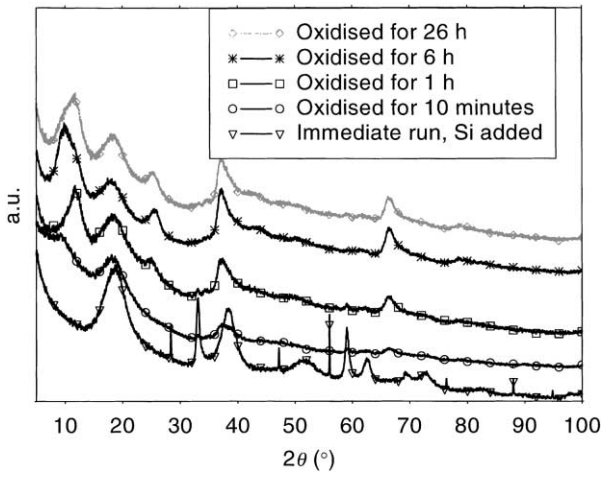

Fig. 2. The extent of oxidation of synthesised β-Ni(OH)$_2$ was followed by XPD measurements. OCl^-(aq) was used as oxidant. Si was added in the "immediate run" in order to correct for the zero point error. The peaks at about 10 and 25° in 2θ may belong to another phase, the γ-phase, different from the conventional hexagonal β-phase, or may be included and indexed as an orthorhombic cell as indicated in the text.

Table 3
Diffraction data for synthetic β-NiOOH with eight observed and nine calculated lines[a]

N	H	K	L	$2\theta_{obs}$	$2\theta_{calc}$	$\Delta 2\theta$
1	1	0	0	11.597	11.783	−0.186
2	0	1	0	18.504	18.363	0.141
3	1	0	1	25.237	25.342	−0.105
4	0	2	0	37.151	37.219	−0.068
5	3	0	1	42.849	42.676	0.173
6	0	1	2	49.583	49.576	0.007
7	5	0	1	66.504	66.544	−0.040
8	5	2	1	78.935	78.792	0.143
9	6	1	0		79.018	−0.083

[a] Double indexed lines shown with the observed 2θ at the closest calculated position. Unit cell used to derive the calculated line positions: orthorhombic crystal system, $a = 7.50(2)$, $b = 4.83(2)$ and $c = 3.97(1)$ Å. $\Delta 2\theta = 2\theta_{obs} - 2\theta_{calc}$.

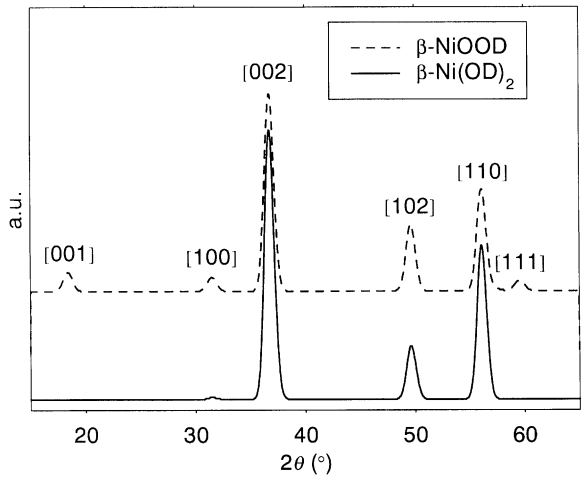

Fig. 3. The appearance of theoretical calculated neutron diffraction patterns for charged and discharged battery Ni material. The positional parameters for β-$Ni(OD)_2$ is given by Greaves and Thomas [8]. Identical theoretical models are used for both charged and discharged masses, only the occupancy of D is changed (from 2 to 1). The two patterns are on an arbitrary intensity scale.

do not change significantly, except that the conventional γ-phase peaks at about 10 and 25° increase in intensity and that the peak position at about 10° in 2θ is not constant and shifts randomly indicating time-dependent effects. The β-$Ni(OH)_2$ [0 0 1] peak, however, does only shift slightly to lower angles indicating a slight expansion of the c-axis.

The discussion above indicates that the conventional γ-phase can be interpreted not only as an expanded c-axis, but also as mentioned before being a consequence of an increased disorder in the ab-plane with the length of the c-axis remaining essentially constant. The XPD pattern, as shown in Fig. 2, may be interpreted as one phase, a corroded β-phasoid, and indexed using DICVOL91 [12] with an orthorhombic cell with the following cell parameters: $a = 7.50(2)$, $b = 4.83(2)$ and $c = 3.97(1)$ Å (see Table 3 for more details).

It must be emphasised that several different cells can be obtained using different acceptance limits of when a peak should be considered as indexed or not. The presupposed information that the length of one of the cell axis should be approximately as long as the c-axis of the β-$Ni(OH)_2$ is fulfilled with the above cell. However, one can also obtain cells with no obvious relations to the unit cell of the discharged phase. Indexing and unit cell determination are far from unique with data as from the present samples.

It should also be emphasised that the peak position at about 10° in 2θ exhibits intensity in all charged battery samples as well, but far from that significance as shown for the synthesised compound.

3.2. NPD measurements

3.2.1. The effect of deuterium and hydrogen

In Fig. 1a and b, the appearance of the neutron diffraction pattern for charged and discharged battery material is shown and compared with XPD diffraction patterns. In all patterns, the contributions from graphite has been subtracted. The battery material is the same as was studied by XPD and has been charged/discharged 10 times in concentrated 6.3 M NaOD heavy water solution.

As can be noted the [0 0 1], [1 0 0] as well as the [1 1 1] peak is absent (or not easily detected) from the NPD pattern when the mass is in the discharged state. This is in accordance with theoretical calculations (cf. Fig. 3). Considering the [0 0 1] peak, it shows intensity mainly when H is present in the structure. The intensity disappears as the ratio between D and H in the compound exceeds 90% of D. This extinction is due to the positions of the atoms in the crystal and the destructive interference originating from Ni, O and D. The structure factor F[0 0 1] is then accidentally very small for this structure and composition $Ni(OD)_2$. Removing one D from β-$Ni(OD)_2$, giving a compound with the stoichiometry NiOOD, retains some intensity to the [0 0 1], [1 0 0] and the [1 1 1] peaks again. Theoretically, this is shown in Fig. 3, and in the charged battery material the same phenomenon appears (the intensity of [1 0 0] is probable buried in the amorphous background) (cf. Fig. 1). This indicates that the charged state actually exhibits a stoichiometry of NiOOD. However, the simultaneous occurrence of NiO_2 is difficult to separate from NiOOD.

Neutron diffraction measurements were also performed on battery material only cycled twice in a NaOD heavy water solution. If β-$Ni(OH)_2$ is transformed to β-NiOOD by a diffusion process of protons to the electrolyte, where H is exchanged by D, a theoretical value of 75% D in the lattice is possible supposing the efficiency being 100%. The discharged material cycled only twice shows intensity of the [0 0 1] peak, corresponding to 65% D of the total concentration of H and D in the lattice. After being cycled 10 times in concentrated flooded NaOD a maximum of 3% of H should theoretically remain in the lattice. From this material

it was not possible to observe any intensity from the [0 0 1] peak and the background intensity had decreased significantly in the NPD patterns. Both of these observations indicate a considerable decrease in the H content. The charged material has a significantly higher background than the discharged one, since the structural information adds to the amorphous background in the charged material.

The discussion above supports the well accepted proton diffusion mechanism previously suggested [13]. However, in a recently published paper [14] cyclic voltametry, using a carbon paste electrode of the battery material, indicates that the solid state mechanism during charge/discharge may be more complicated than a single step reaction and include several not yet well defined steps.

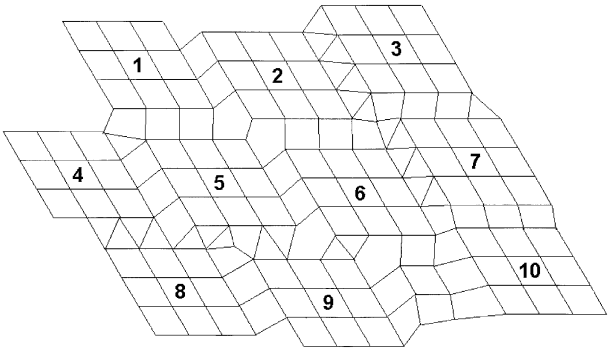

Fig. 4. Hypothetical view of ten regions of 3 × 3 unit cells in the *ab*-layer of $Ni(OH)_2$ linked together.

3.2.2. Comparison of the results with XRD

The NPD [1 1 0] peak at $2\theta \approx 62^\circ$ shown for charged material in Fig. 1a and b should not be a rest from discharged material since the discharged [1 1 0] peak is positioned at a lower 2θ value. A theoretical calculation shows that [1 1 0] should be present in the NDP pattern for both charged and discharged material (cf. Fig. 3). It should be mentioned that the same structural model for both discharged and charged materials are the structure model for β-$Ni(OD)_2$ proposed by Greaves and Thomas [8] with the only difference being the deuterium content. Thus no peak shifts are modelled in the diffraction patterns when the charged and discharged samples are compared, only intensity differences. The peak at $2\theta \approx 66^\circ$ in the charged material should be indexed as [1 1 1] rather than [1 1 0], since the appearance of these peaks in NPD exhibits the same appearance and approximately the same 2θ-difference as the corresponding XPD peaks of the discharged state. The only difference is a small shift in 2θ but this may be attributed to slight variations in the cell parameters (cf. Fig. 1).

In discharged state the [1 1 1] NPD peak disappears, which is in accordance with theoretical calculations (cf. Fig. 3). Using information from both the NPD and XPD we can be much more confident about the indexing.

The NPD patterns of discharged and charged materials were indexed using four peaks for the charged state and eight peaks for the discharged state. The cell parameters were refined using the program PUDER [5]. This calculations resulted in a hexagonal cell with $a = 2.98(1)$ Å (charged); 3.128(2) Å (discharged) and $c = 4.69(7)$ Å (charged); 4.66(2) Å (discharged).

The cell parameters for the charged phase are in the same order as extracted from the XPD measurements. The parameters for the discharged phase is identical with those extracted from the XPD measurements in this work and also with observed values in our earlier work [15].

The diffraction experiments above indicate a very close similarity between the charged and the discharged structures. We postulate that the two structures mainly differ in an increased disorder in the *ab*-plane. The lack of structural long range order in the *ab*-plane may be due to a collapse of the order of the domains that build up the particles (Fig. 4). The physical background to this collapse can be induced distortions of the Ni–O octahedra [16] and introduction of strains in the structure occurring when Ni is oxidised. These rearrangements may also affect the distance in the *c*-direction in a similar way as the turbostratic structure of graphite does, that is, a somewhat longer *c*-axis compared to the discharged state should be observed, due to a disordered stacking through random rotations or displacements of ordered layers. This is in accordance with the observation of a slight expansion of the *c*-axis in this work. The increased valence in the charged state compared with the discharged state should probably not give an extended *c*-distance as the result, if each layer is electrically neutral. Rather a contraction of the *c*-axis due to close contacts and the possibility of forming hydrogen bonds should occur between Ni–OH and O–Ni. A schematic 2D-view is shown in Fig. 5.

3.3. Radial distribution functions

The reduced radial distribution function is used to characterise amorphous samples and can be expressed as:

$$G(r) = 4\pi r[\rho(r) - \rho_0] \quad (3)$$

where r is the atom–atom distance, $\rho(r)$ is the atomic density at distance r and ρ_0 is the average atomic density. The

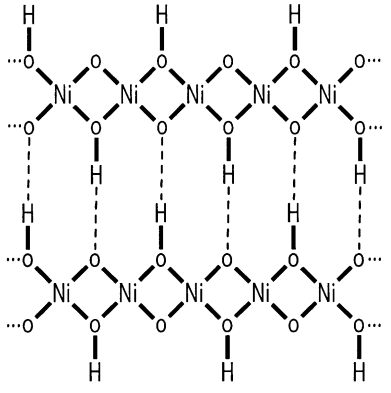

Fig. 5. Schematic 2D-view of a possible model of attraction between two NiOOH layers with the formation of hydrogen bonds.

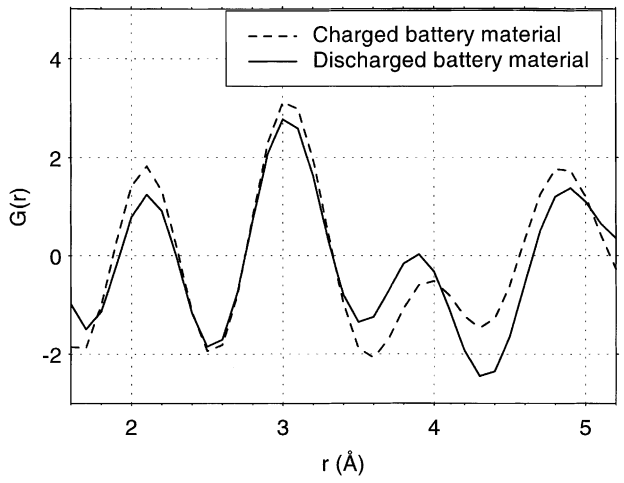

Fig. 6. Radial distribution functions of charged and discharged battery Ni material, based on X-ray diffraction data, originating from the material that been cycled 10 times in heavy water alkali solution.

resulting peaks indicate the most frequently occurring atom–atom distances in the lattice. Experimentally, the RDF is found as the Fourier transform of the interference function, $i(s)$, which is the structurally dependent part of the diffraction data. These data can be found from the experimental intensities suitably corrected for background intensities (in this special case the background: graphite, tape and air) absorption, polarisation effects, incoherent scattering, multiple scattering and instrumental effects. The resulting structure dependent scattering was scaled with the "high-angle method" where $I_{\text{coherent}} + I_{\text{incoherent}}$ is compared with I_{observed} [17].

Fig. 6 shows the resulting RDF calculations of discharged and charged battery materials, calculated on the material that had been charged/discharged 10 times. Only XPD data was used to calculate the radial distribution function. The dominant atom–atom distances in the charged and discharged structures are ≈2 Å (interpreted as Ni–O distance), which is in accordance with EXAFS measurements, and ≈3 Å (unit cell *ab*-distances). Further indication of the ease with which the layers form are that in freshly precipitated β-$Ni(OH)_2$ the 3 Å distance immediately appears in the diffraction pattern as the two reflections [1 0 0] and [1 1 0] indicating that the lattice is initially growing in the *ab*-direction (cf. Fig. 7). The 3 Å nearest neighbour distance is also visible from RDF calculations of freshly precipitated β-$Ni(OH)_2$. The peak at around 5 Å in Fig. 6 may be interpreted as the distance in the *c*-direction but it should be emphasised that accurate correction procedures are necessary for producing reliable results at high *r*-values. Preferably one would like to have an experimental set-up that eliminates the incoherent scattering experimentally. These set-up were not available to the authors of the present work. The absolute values of the RDF calculations in the present work may be incorrect on an absolute scale, but since identical experimental and evaluation procedures were performed we do not hesitate to the correctness of the results on a relative basis.

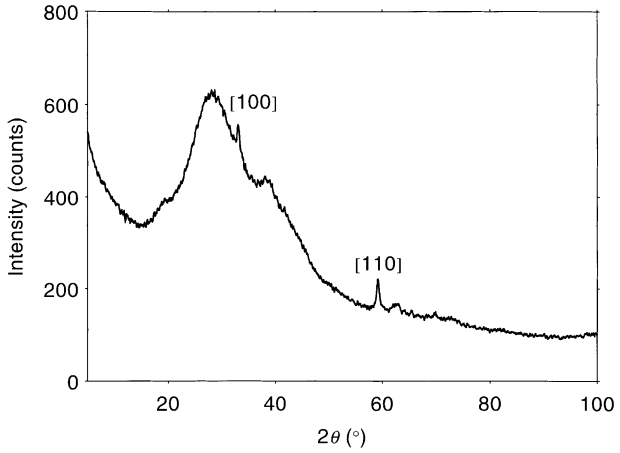

Fig. 7. The appearance of the X-ray diffraction pattern of fresh precipitated β-$Ni(OH)_2$.

3.4. Comparison between RDF calculations and XPD patterns

The structural ordering along the *ab*-plane is destroyed in the charged state, which has been indicated by XPD measurements ([1 0 0] and [1 1 0] peaks are absent). Still the 3 Å distance, the [1 0 0] distance, is dominant as seen from the RDF calculations. Modelling the *ab*-plane as broken up into small islands, mentioned above, enables both of these observations to be fitted with the same simple model. The rearrangement of the domains make the dimensions of the physical particles much larger than the coherently scattering domains, yielding severe diffraction line broadening.

4. Conclusions

1. The discharged Ni electrode material attains a high degree of disorder in the *ab*-plane, and a largely unaffected *c*-axis as the material is charged. Despite these differences the diffraction experiments together with RDF calculations indicate a close similarity between the charged and the discharged average local structures, and experimental results point toward a model of the charged phase consisting of disordered domains in the *ab*-plane.
2. A reassignment of indices to the few visible peaks of the charged phase has been done for the X-ray and neutron diffraction patterns to correspond more closely to the discharged structural model. An NPD pattern consisting of four peaks from the charged phase was used for indexing and refinement of cell parameters; hexagonal cell with $a = 2.98(2)$, $c = 4.72(7)$ Å.
3. The conventional γ-phase is in this paper interpreted as being formed due to high disorder in the *ab*-plane and should thus perhaps not be considered as a phase of its own, but more as one of many similar modifications of the β-NiOOH structure, that in its turn also should be

considered as a slight modification of the β-$Ni(OH)_2$ structure. Small structural deviations interconvert the different ''phases''. The fact that small structural effects should be involved are supported by the easy interconvesion of the charged and discharged phases essentially by solid state reactions and hydrogen diffusion.

Acknowledgements

Division of Inorganic Chemistry, Stockholm University, Sweden is acknowledged for financial support.

References

[1] H. Bode, K. Dehmelt, J. Witte, Electrochim. Acta 11 (1966) 1079.
[2] Rundlöf, H., Personal Communication, NFL, Studsvik, Sweden.
[3] Vogel, A.I., A Textbook of Quantitative Inorganic Analysis, 3rd Edition, Longman, New York, 1961.
[4] J. McBreen, W.E. O'Grady, K.I. Pandya, R.W. Hoffman, D.E. Sayers, Langmuir 3 (1987) 428.
[5] Eriksson, L., Personal Communication, Computer Program PUDER, Stockholm University, Stockholm, 2001.
[6] S. Debate, F. Fourgeot, F. Henn, J. Power Sources 87 (2000) 125.
[7] C. Tessier, P.H. Haumesser, P. Bernard, C. Delmas, J. Electrochem. Soc. 146 (1999) 2059.
[8] C. Greaves, M.A. Thomas, Acta Cryst. B 42 (1986) 51.
[9] D. Singh, J. Electrochem. Soc. 145 (1998) 116.
[10] O. Glemser, J. Einerhand, Z. Anorg, Allg. Chem. 261 (1950) 43.
[11] B.C. Cornilsen, P.J. Karjala, P.L. Loyselle, J. Power Sources 22 (1988) 351.
[12] A. Boultif, D. Louër, J. Appl. Cryst. 24 (1991) 987.
[13] E.A. Charles, The effects of cobalt hydroxide addition on the nickel hydroxide electrode, Ph.D. Thesis, University of Newcastle upon Tyne, Newcastle, 1989.
[14] E. Ahlberg, U. Palmqvist, N. Simic, R. Sjövall, J. Power Sources 85 (2000) 245.
[15] U. Palmqvist, L. Eriksson, J. García-García, N. Simic, E. Ahlberg, R. Sjövall, J. Power Sources 99 (2001) 15–25.
[16] K.I. Pandya, R.W. Hoffman, J. McBreen, W.E. O'Grady, J. Electrochem. Soc. 137 (1990) 383.
[17] V. Petkov, J. Appl. Cryst. 22 (1989) 387.